

${}^7\text{Li}$ and ${}^7\text{Be}$ production in the $\alpha + \alpha$ reaction*

C. H. King, Sam M. Austin, H. H. Rossner,[†] and W. S. Chien

Cyclotron Laboratory and Physics Department, Michigan State University, East Lansing, Michigan 48824

(Received 20 June 1977)

Differential cross sections for the ${}^4\text{He}(\alpha, p)$ reaction leading to the ground and 478-keV states of ${}^7\text{Li}$ have been measured at 11 energies between 39.0 and 49.5 MeV and used to determine integral cross sections for ${}^7\text{Li}$ production in ${}^4\text{He}(\alpha, p)$. Comparison of the ground state cross sections with ${}^7\text{Li}(p, \alpha)$ data using the principle of detailed balance indicates good agreement with the most recent ${}^7\text{Li}(p, \alpha)$ measurements but not with some older results. Cross sections for ${}^4\text{He}(\alpha, d){}^6\text{Li}$ (ground state), extracted at three energies, are consistent with the most recent ${}^6\text{Li}(d, \alpha)$ measurements. Cross sections for ${}^7\text{Be}$ production via ${}^4\text{He}(\alpha, n){}^7\text{Be}$ were determined at nine energies between 39.4 and 47.4 MeV by direct collection of the ${}^7\text{Be}$ and detection of the γ rays following its decay. These cross sections are essentially identical to the ${}^7\text{Li}$ production cross sections above 43 MeV but are smaller below this energy because of threshold effects. The ${}^4\text{He}(\alpha, p)$ and ${}^4\text{He}(\alpha, n)$ reactions are involved in several mechanisms which have been proposed to explain the universal abundance of ${}^7\text{Li}$, and calculations of these processes have assumed cross sections larger than our data. We therefore confirm earlier conclusions that ${}^7\text{Li}$ is unlikely to be produced by galactic cosmic-ray spallation alone, but the status of the other mechanisms remains unclear. Peaks in the ${}^4\text{He}(\alpha, p)$ and ${}^4\text{He}(\alpha, n)$ excitation functions are discussed in terms of resonances in ${}^8\text{Be}$. Parameters determined by Kumar and Barker in a fit to ${}^7\text{Li}(p, \alpha)$ data are inadequate to explain our ${}^4\text{He}(\alpha, p){}^7\text{Li}$ (478 keV) cross sections.

NUCLEAR REACTIONS ${}^4\text{He}(\alpha, p)$, $E = 39.0\text{--}49.5$ MeV; measured $\sigma(E; \theta, E_p)$, $\sigma(E)$. ${}^4\text{He}(\alpha, n)$, $E = 39.4\text{--}47.4$ MeV; measured $\sigma(E)$. ${}^4\text{He}(\alpha, d)$, $E = 46.7\text{--}49.5$ MeV; measured $\sigma(E; \theta)$, $\sigma(E)$. Astrophysical implications for ${}^7\text{Li}$ production considered. Discussion of ${}^8\text{Be}$ levels in R -matrix formalism.

I. INTRODUCTION

The observed abundances of the nuclides with $A \geq 12$ can be explained remarkably well by assuming that they were created through chains of nuclear reactions in stellar interiors.¹ However, creation of the lighter nuclides seems to require for the most part an alternative mechanism. This is particularly true of deuterium and the isotopes of lithium, beryllium and boron, which are too fragile to survive in the hot environment of stellar interiors. Although the abundance of these nuclides is very low, the explanation of their origin can have significant consequences for our understanding of the universe. For example, in the case of deuterium it appears that no realistic process other than a primordial big bang can produce this nuclide in sufficient amounts to explain the observed abundance.² This result implies that most of the deuterium in the universe is of cosmological origin,^{2,3} a conclusion which suggests that the universe is open.

A likely mechanism for the creation of several of the light elements is the spallation of interstellar matter by cosmic rays. Calculations of the production rates in this process indicate that ${}^6\text{Li}$ and the stable beryllium and boron isotopes can be produced in approximately sufficient amounts. However, ${}^7\text{Li}$ appears to be significantly underproduced,^{4,5} although the calculations for this isotope contain substantial uncertainties. Since significant amounts of ${}^7\text{Li}$ can also be created in a big bang,³ the abundance of this isotope might provide an additional constraint on the nature of the universe if non-cosmological mechanisms should prove insufficient.

The principal source of ${}^7\text{Li}$ in cosmic-ray spallation is the interaction between ${}^4\text{He}$ in cosmic rays and ${}^4\text{He}$ in the interstellar medium. This interaction can produce ${}^7\text{Li}$ directly via the ${}^4\text{He}(\alpha, p)$ reaction to one of the two

particle-stable states of ${}^7\text{Li}$: the ground state and the first excited state (478 keV). In addition, since ${}^7\text{Be}$ decays to ${}^7\text{Li}$ by electron capture, the reaction ${}^4\text{He}(\alpha, n)$ to the two analogous states in ${}^7\text{Be}$ (ground state and 429 keV state) also contributes to the net production of ${}^7\text{Li}$. Until recently very few direct measurements of the cross sections in these four channels were available. Instead, in the spallation calculations^{4,5} the cross sections for the ${}^4\text{He}(\alpha, p)$ reaction to the ${}^7\text{Li}$ ground state were inferred by detailed balance from measured ${}^7\text{Li}(p, \alpha)$ cross sections. Assumptions were then made about the cross sections in the other three channels. The uncertainty in the calculated ${}^7\text{Li}$ production was further enhanced by substantial discrepancies in measurements of the ${}^7\text{Li}(p, \alpha)$ cross sections.

Because of their potential importance for understanding the origin of ${}^7\text{Li}$, we have measured the relevant $\alpha + \alpha$ cross sections for α energies from just above threshold (34.7 MeV for ${}^4\text{He}(\alpha, p)$ and 38.0 MeV for ${}^4\text{He}(\alpha, n)$) up to 50 MeV. This energy region is particularly important, since the cross sections are largest at these low energies, and some models for cosmic-ray spallation⁴ assume the cosmic-ray flux to be large at low energies as well. Other mechanisms which have been proposed for ${}^7\text{Li}$ production (considered in Sec. IV B) are also sensitive to the low-energy $\alpha + \alpha$ cross sections. The experimental procedure and data reduction for the ${}^4\text{He}(\alpha, p)$ reaction are described in Sec. II of this paper and those for the ${}^4\text{He}(\alpha, n)$ reaction in Sec. III. The possible astrophysical implications of these measurements are discussed in Sec. IV. In the energy range covered by the present experiments peaks appear in the excitation functions which can be interpreted as resulting from resonances in the compound nucleus ${}^8\text{Be}$. Information obtained about the structure of ${}^8\text{Be}$ is described in Sec. V. Finally, a summary of our results and conclusions is provided in Sec. VI. A

preliminary report of these experiments has appeared previously.⁶

II. THE REACTION ${}^4\text{He}(\alpha, p){}^7\text{Li}$

A. Experimental procedure

Cross sections for the ${}^4\text{He}(\alpha, p)$ reaction were determined from measurements of the angular distributions of the outgoing protons. The target was a 12.7-cm diameter cylindrical cell with windows of 0.025-mm thick Kapton and filled with helium gas to approximately atmospheric pressure. The pressure and temperature of the cell were monitored throughout the experiment to determine the effective target thickness. Outgoing particles were detected in two silicon surface-barrier detectors fixed 30° apart, and placed behind a double-slit collimator system.

Because of the small number of possible two-body final states in the $\alpha + \alpha$ reaction and the low three-body background in this energy range, particle identification was unnecessary. A sample spectrum is shown in Fig. 1. The resolution was dominated by kinematic broadening, and was typically about 75 keV full width at half maximum, allowing the peaks of interest to be well resolved. The presence of identical particles in the entrance channel forces the differential cross sections for all outgoing channels to be symmetric about 90° in the center-of-mass reference frame. Thus, measurements were mainly confined to center-of-mass angles less than 90° .

B. Data analysis

Since in most cases the peaks were well resolved, the yields could be determined by simply subtracting away the background. In the few cases where the peaks overlapped, a gaussian fitting procedure was used to extract the areas. The differential cross sections at three representative energies are shown in Fig. 2.

Because these measurements were made at energies close to the reaction threshold, the differential cross sections can be characterized in terms of a Legendre polynomial expansion involving only a few terms. In addition, the identical particle symmetry limits the expansion to Legendre polynomials of even order:

$$\frac{d\sigma}{d\Omega} = \frac{\sigma}{4\pi} \sum_{L=0}^{L_{\max}} B_L P_L(\cos\theta) \quad (1)$$

L even

with $B_0 \equiv 1$. Adequate fits in this energy range could be obtained with $L_{\max} = 6$.

The integral cross section σ and the coefficients B_L determined by this procedure are shown in Figs. 3 and 4. The integral cross sections are also listed in Table I. The uncertainties shown for the B_L include contributions from counting statistics and uncertainties in the fits to the angular distribution. Those quoted for the integral cross section are total uncertainties, containing not only statistical contributions, but also systematic uncertainties in the determination of the detector collimator geometry, in the temperature and the pressure of the target gas, in the integrated beam current, and in the detector angle. All these uncertainties were added in quadrature and typically amount to about 5%, with the statistical contributions usually negligible compared to the rest. The energies listed in the table and shown in the figures correspond to the measured beam energy corrected for energy loss in the front window of the gas cell and in the helium gas from the front to the center of the cell.

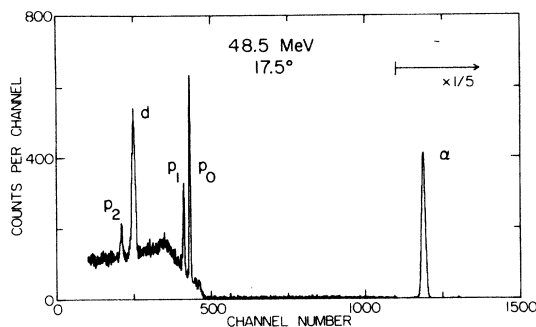


FIG. 1. Particle spectrum from the $\alpha + \alpha$ reaction at 48.5 MeV incident laboratory energy and 17.5° laboratory scattering angle. The elastic scattered α -particle group is labeled " α ", the deuteron group from the ${}^4\text{He}(\alpha, d){}^6\text{Li}(\text{g.s.})$ reaction is labeled " d ", and the proton groups from the ${}^4\text{He}(\alpha, p)$ reaction leading to the ground, 0.478-MeV, and 4.633-MeV states of ${}^7\text{Li}$ are labeled " p_0 ", " p_1 ", and " p_2 ", respectively.

C. Comparison to other data

Two other determinations of ${}^4\text{He}(\alpha, p)$ cross sections to the ground and 478 keV states of ${}^7\text{Li}$ have been reported in the literature. Burcham *et al.*⁷ measured the cross sections at $E_\alpha = 38.5$ MeV. Recently Slobodrian⁸ has reported cross sections for incident α -particle energies between 37.5 and 43.0 MeV, derived from spectra taken in the $\alpha + \alpha$ elastic scattering measurements of Conzett *et al.*⁹ These cross sections are shown in Fig. 5 together with our data, and the agreement among the measurements is generally good.

The cross section for ${}^4\text{He}(\alpha, p){}^7\text{Li}(\text{g.s.})$ can also be compared with existing ${}^7\text{Li}(p, \alpha){}^4\text{He}$ data by using the principle of detailed balance. Numerous measurements of ${}^7\text{Li}(p, \alpha)$ angular distributions have been made,¹⁰ but large discrepancies exist among the various determinations of the absolute cross sections.^{1, 12, 13} The situation is complicated by the fact that in many cases quoted values for the integral cross sections fail to properly account for the fact that the two particles in the final state are identical.¹³ For a reaction with two identical particles in the final channel the integral cross section is related to the differential cross section via

$$\sigma = 1/2 \int \frac{d\sigma}{d\Omega} d\Omega,$$

where the factor of 1/2 prevents double counting of the particles in the final state so that σ has the usual definition of reaction rate per incident flux.

The most complete ${}^7\text{Li}(p, \alpha)$ data in the energy range of concern here are those of Cassagnou *et al.*¹⁴ for $E_p \leq 4.8$ MeV and Mani *et al.*¹⁵ for $E_p = 4-12$ MeV. The angular distributions for both sets of measurements have been fitted to Eq. (1) by Mani *et al.* Terms up to eighth order were used in the fits, but the resulting B_8 coefficients were consistent with zero. The absolute cross sections for these data were normalized to measurements made by Freeman *et al.*¹⁶ below 1.5 MeV. However, more recent measurements¹¹ of absolute ${}^7\text{Li}(p, \alpha)$ cross sections at 1.36 MeV disagree with the Freeman *et al.* data, being approximately a factor of two smaller (ranging from 40% to 65% of the Freeman *et al.* measurements). In addition, measurements of these cross sections by Kilian *et al.*¹⁷ between 2.7 and 10.6 MeV are also approximately a factor

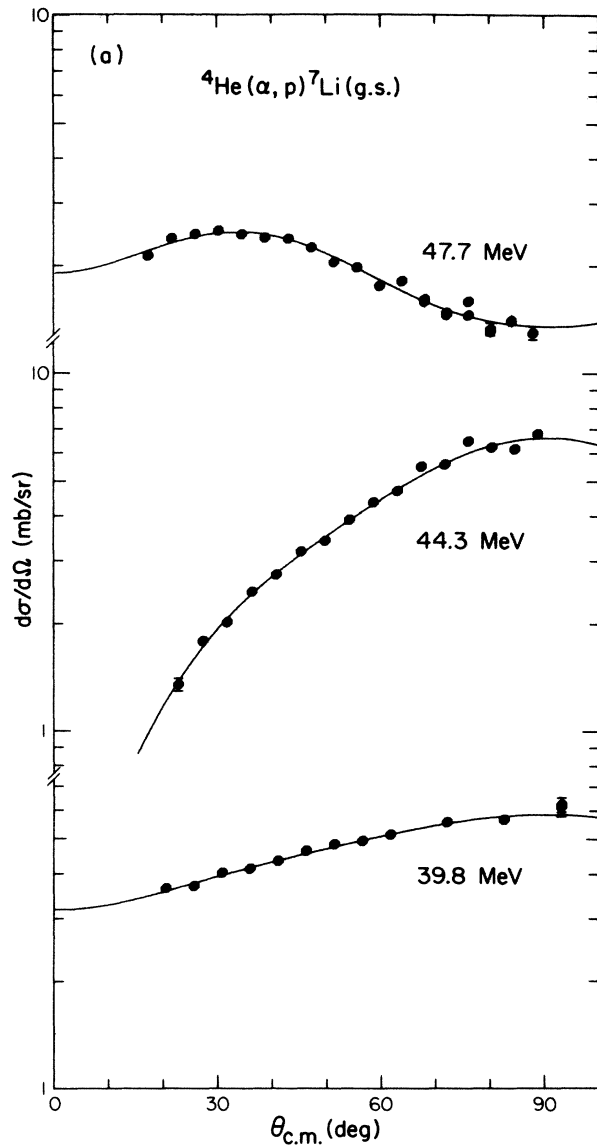


FIG. 2a. Differential cross sections for ${}^4\text{He}(\alpha, p)$ leading to the ground state of ${}^7\text{Li}$ at incident laboratory energies of 39.8, 44.3, and 47.7 MeV. The lines indicate the least-squares fits to these cross sections using the Legendre polynomial expansion of Eq. (1) with $L_{\text{max}} = 6$.

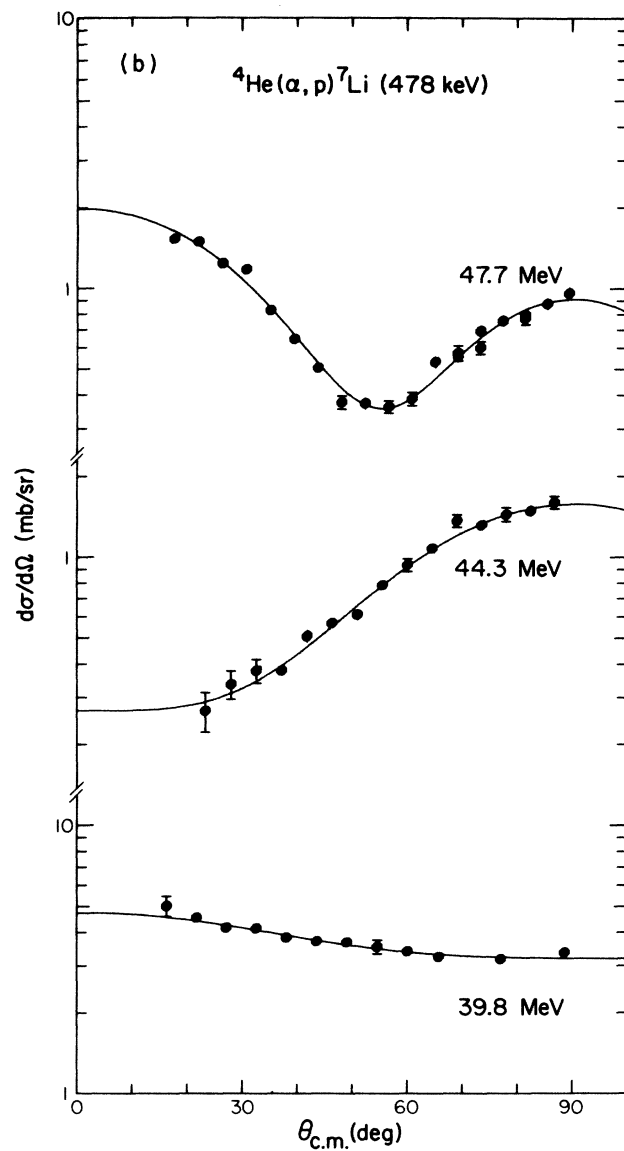


FIG. 2b. Differential cross sections for ${}^4\text{He}(\alpha, p)$ leading to the first excited state (478 keV) of ${}^7\text{Li}$. See caption to Fig. 2a for further explanation

of two smaller than the numbers quoted by Mani et al. when the fact that the final state particles are identical is properly taken into account (see Ref. 13). We therefore follow Kumar and Barker¹² in assuming that the absolute cross sections given in Mani et al. should be reduced by a factor of two.

Some modifications of the usual detailed-balance expressions are also required in the case where identical particles are involved. The reciprocity theorem states that a T-matrix element and the matrix element obtained from it by applying the time-reversal operator are equal. This theorem holds for properly symmetrized T-matrix elements.¹⁸ Hence, despite the presence of identical particles, the detailed-balance expression for spin-aver-

aged differential cross sections takes on the usual form¹⁹

$$\frac{\frac{d\sigma}{d\Omega}(A + B \rightarrow C + D)}{\frac{d\sigma}{d\Omega}(C + D \rightarrow A + B)} = \frac{\hat{S}_C \hat{S}_D k_{CD}^2}{\hat{S}_A \hat{S}_B k_{AB}^2}$$

where $\frac{d\sigma}{d\Omega}(A + B \rightarrow C + D)$ is the differential cross section for the reaction $A + B \rightarrow C + D$; $\hat{S}_A \equiv 2S_A + 1$, with S_A the spin of particle A; and $\hbar k_{AB}$ is the relative momentum in the $A + B$ channel. This implies, for example, that the angular-distribution coefficients B_L will be the same for

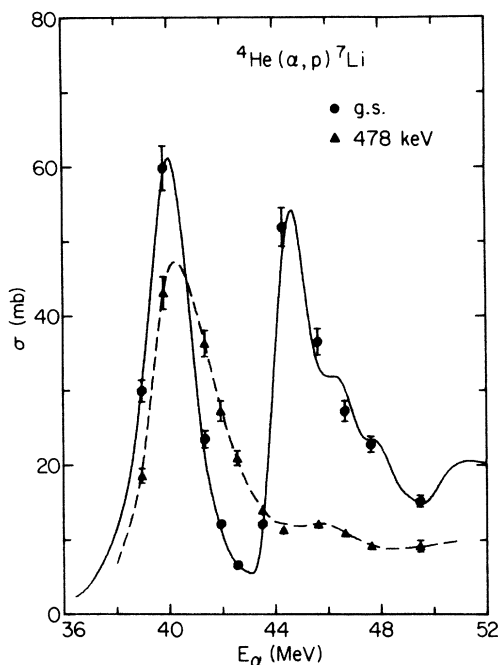


FIG. 3. The integral cross sections σ for ${}^4\text{He}(\alpha, p)$ leading to the ground state (circles) and first excited state (triangles) of ${}^7\text{Li}$. The solid line represents the detailed-balance predictions for ${}^4\text{He}(\alpha, p){}^7\text{Li}$ (g.s.) based on the cross sections of Mani *et al.*¹⁵ for ${}^7\text{Li}(p, \alpha)$ divided by 2. The dashed line is to guide the eye through the points for the ${}^4\text{He}(\alpha, p){}^7\text{Li}$ (478 keV) reaction.

${}^4\text{He}(\alpha, p)$ to the ${}^7\text{Li}$ ground state and for ${}^7\text{Li}(p, \alpha)$. For the case of integral cross sections, factors of 2 arise in order to avoid double counting of particles as described above. Thus,²⁰

$$\frac{\sigma(A+B+C+D)}{\sigma(C+D+A+B)} = \frac{(1+\delta_{AB})\hat{S}_C\hat{S}_Dk^2}{(1+\delta_{CD})\hat{S}_A\hat{S}_Bk^2}. \quad (2)$$

The ground state ${}^4\text{He}(\alpha, p)$ angular-distribution coefficients are compared with those of Mani *et al.* for ${}^7\text{Li}(p, \alpha)$ in Fig. 4 and the agreement between the two is good. As indicated above, the ${}^7\text{Li}(p, \alpha)$ integral cross sections of Mani *et al.* are believed to be too large by a factor of 2. We have therefore divided them by 2 before inserting into Eq. (2) to obtain the detailed-balance predictions for the ${}^4\text{He}(\alpha, p){}^7\text{Li}$ (g.s.) integral cross sections shown in Fig. 3. Our data agree well with these predictions and thus with the more recent determinations of ${}^7\text{Li}(p, \alpha)$ cross sections.^{11,17}

D. The reaction ${}^4\text{He}(\alpha, d){}^6\text{Li}$

In the experiment described in Sec. II B, the deuteron group from the ${}^4\text{He}(\alpha, d)$ reaction leading to the ground state of ${}^6\text{Li}$ was observed at 46.7, 47.7, and 49.5 MeV. The differential cross sections for this ${}^4\text{He}(\alpha, d)$ reaction were extracted, and least-squares fits to these data were made using Eq. (1) with $L_{\text{max}} = 4$. The resulting integral cross sections σ are shown in Fig. 6.

These cross sections can be compared with measurements of the cross sections for the inverse reaction ${}^6\text{Li}(d, \alpha)$ using the principle of detailed balance. Unfortunately, as for the ${}^7\text{Li}(p, \alpha)$ reaction, various measurements of ${}^6\text{Li}(d, \alpha)$ have yielded large discrepancies in the absolute

cross section determinations. As can be seen in Fig. 6, our measurements are in reasonable agreement with those of McClenahan and Segel²¹ but differ from those of Jeronimo *et al.*²² by more than a factor of two. The values of B_2 and B_4 extracted from our angular distributions agree reasonably well with those reported by both Jeronimo *et al.* and McClenahan and Segel. Comparison of these with other ${}^6\text{Li}(d, \alpha)$ measurements is given in Ref. 21.

III. THE REACTION ${}^4\text{He}(\alpha, n){}^7\text{Be}$

A. Experimental procedure

Accurate differential cross sections are considerably more difficult to determine from measurements of angular distributions of neutrons than from measurements of angular distributions of charged particles because of the difficulties of neutron detection. However, the quantities of particular astrophysical interest are the total ${}^7\text{Be}$ production cross sections rather than the differential cross sections. Thus, we have chosen a method which allows us to measure the total production cross sections directly. Such a measurement is feasible for the ${}^4\text{He}(\alpha, n){}^7\text{Be}$ reaction because the ${}^7\text{Be}$ ions are confined to extreme forward angles ($<11^\circ$ for $E_\alpha < 50$ MeV). Thus, all ${}^7\text{Be}$ ions produced in the reaction can be collected at one time in a foil placed behind the target. A determination of the number N of ${}^7\text{Be}$ collected then yields the cross section for ${}^7\text{Be}$ production in both of its two particle-stable states (ground state and 429-keV state). Most of the ${}^7\text{Be}$ nuclei decay directly to the ${}^7\text{Li}$ ground state, but there is a branch to the first-excited state of ${}^7\text{Li}$ at 478 keV (the weighted average of the branching ratios given in Ref. 10 is $10.4 \pm 0.1\%$). The measurement of the 478 keV γ rays accompanying this branch can be used to determine the ${}^7\text{Be}$ decay rate dN/dt and hence to determine N .

The target was a gas cell with a 2.5 cm nominal diameter, 0.011-mm thick Kapton windows, and filled with helium gas to approximately atmospheric pressure. The minimum energy of the outgoing ${}^7\text{Be}$ nuclei produced in the reaction (>14 MeV) is large enough so that none will stop in the helium gas or cell windows. In order to determine the effective target thickness, the pressure and temperature of the gas were monitored during the experiment, and after the experiment the length of the irradiated gas column from entrance to exit window at the appropriate gas pressure was measured. The ${}^7\text{Be}$ ions were stopped in circular pieces of aluminum foil 0.12 mm thick and 5.8 cm in diameter, placed 11.4 cm behind the center of the target.

In order to account for extraneous ${}^7\text{Be}$ ions produced from interactions in the cell windows and in the collecting foil, a direct measurement of this background was made. This was achieved by filling the gas cell with H_2 gas to a pressure with equivalent stopping power for the ${}^7\text{Be}$ ions as the He gas used in the primary measurements. Since no ${}^7\text{Be}$ ions can be produced from reactions in the H_2 gas, the number of ${}^7\text{Be}$ ions collected in the aluminum foil determines the background.

In order to eliminate possible effects on the beam current integration due to small-angle scattering in the aluminum collecting foils the experimental runs were normalized using a monitor detector placed at 45° to measure α -particle elastic scattering from the target He gas. The ratio of the monitor counts to integrated beam current was determined at each energy from measurements without a foil in place.

Measurements with the He gas in the target were made at the nine energies between 39.43 and 47.36 MeV given in Table II. The energies shown have been corrected for energy loss of the beam in the front window of the cell and target gas. The background measurements were made

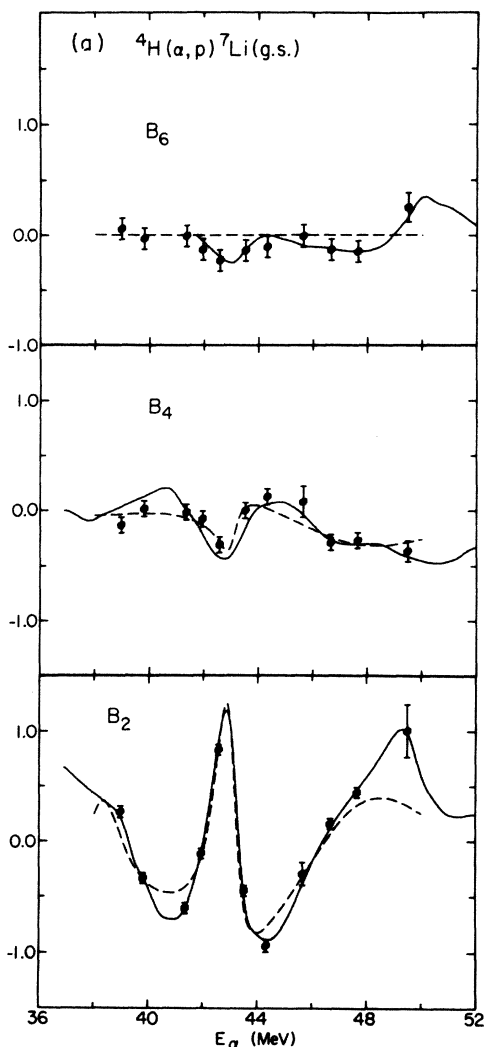


FIG. 4a. Angular distribution coefficients B_L (as defined in Eq. (1)) for the ${}^4\text{He}(\alpha, p){}^7\text{Li}(\text{g.s.})$ reaction leading to the ground state of ${}^7\text{Li}$. The solid lines represent the corresponding angular distribution coefficients for the inverse ${}^7\text{Li}(p, \alpha)$ reaction as measured by Mani *et al.*¹⁵ The dashed lines are predictions for these coefficients based on the ${}^8\text{Be}$ level parameters from the R-matrix fits of Kumar and Barker¹² to ${}^7\text{Li}(p, \alpha)$ cross sections.

at 39.43, 41.67, 43.00, 44.42, and 47.36 MeV, and the yield was found to rise monotonically in this energy range. Therefore the backgrounds for the other four energies were determined by interpolation. The background contribution was less than 12% except at 43.00 MeV (22%) and 47.36 MeV (30%).

Since ${}^7\text{Be}$ has a half-life of 53.3 days, we waited at least two weeks after the irradiations to allow most of the extraneous activity to decay away. The γ activity of the foils was measured several times between 15 and 45 days following irradiation using coaxial Ge(Li) detectors ranging from 40 to 80 cm^3 active volume. Sample spectra are shown in Fig. 7.

The absolute efficiency of the Ge(Li) detectors was determined by placing a calibrated mixed-radionuclide γ -

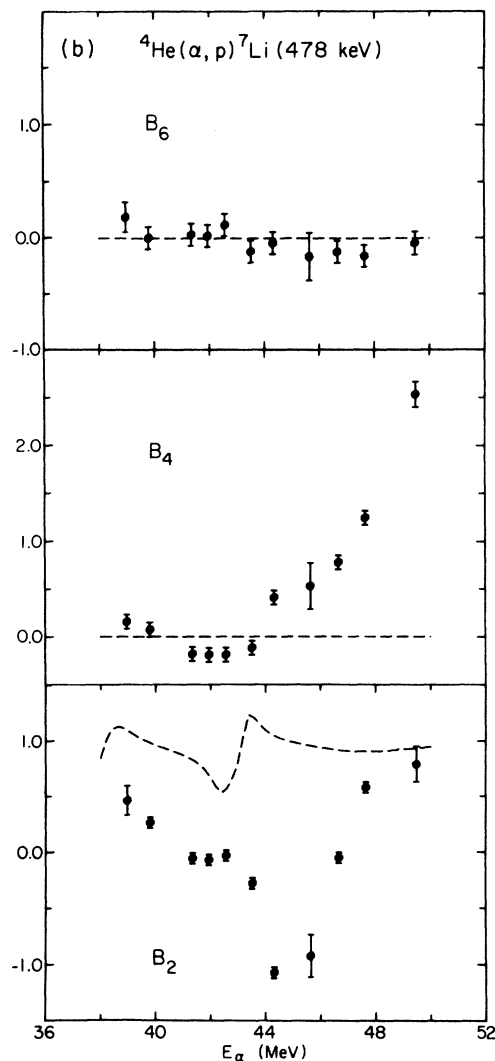


FIG. 4b. Angular distribution coefficients for the ${}^4\text{He}(\alpha, p){}^7\text{Li}(478 \text{ keV})$ reaction leading to the first excited state of ${}^7\text{Li}$. The dashed lines have the same meaning as in Fig. 4a.

ray source²³ at the foil position, 23 cm from the detector. Variations in efficiency for γ rays coming from different parts of the foil were determined empirically by varying the position of the calibrated source. The γ -ray spectra were collected for periods of several hours with the time determined precisely using an electronic timer. The γ -ray yields from the aluminum foils and calibrated source were obtained by fitting the peaks assuming a gaussian shape with exponential tails and a linear background. The cross sections finally obtained are listed in Table II and shown in Fig. 8.

The principal contributions to the uncertainties in the cross sections arise in the determination of the γ -ray activity and of the length of the irradiated gas column. The uncertainty in the activity measurements was determined empirically from measurements made with different γ -detection geometries and from the consistency of measurements made at different times after the irradiation. The uncertainty in the length of the target gas column was about 7%, mostly arising from distortions in

TABLE I. $\alpha + \alpha \rightarrow p + {}^7\text{Li}$ Cross Sections.

E_α (MeV) (± 100 keV)	$\sigma_{\text{g.s.}}$ (mb)	σ_{478} (mb)	σ_{sum} (mb)
38.97	29.9 ± 1.5	18.5 ± 1.0	48.4 ± 2.5
39.80	59.9 ± 3.0	43.1 ± 2.2	103.0 ± 5.2
41.35	23.4 ± 1.2	36.3 ± 1.8	59.7 ± 3.0
41.95	12.0 ± 0.6	27.2 ± 1.4	39.2 ± 2.0
42.57	6.5 ± 0.3	20.8 ± 1.0	27.3 ± 1.4
43.52	12.0 ± 0.6	13.8 ± 0.7	25.8 ± 1.3
44.32	52.0 ± 2.6	11.2 ± 0.6	63.2 ± 3.2
45.64	36.5 ± 1.8	12.0 ± 0.6	48.5 ± 2.4
46.67	27.2 ± 1.4	10.8 ± 0.5	38.0 ± 1.9
47.65	22.7 ± 1.1	9.1 ± 0.5	31.8 ± 1.6
49.49	15.1 ± 0.8	9.1 ± 0.8	24.2 ± 1.6

the cell window due to beam heating effects. Uncertainties in other quantities such as He gas temperature and pressure, integrated beam current, and the half-life and branching ratios of the ${}^7\text{Be}$ decay were negligible. Total uncertainties are typically about 10%.

B. Comparison to other data

One other attempt to determine the ${}^7\text{Be}$ production cross sections was made some time ago at 39.0 MeV by Walker, Link, and Smith²⁴. No evidence for ${}^7\text{Be}$ production was found, and their upper limit on the cross section was 0.7 mb, considerably smaller than one would estimate from a naive extrapolation of our results.

The ${}^4\text{He}(\alpha, n)$ results can also be compared approximately with the ${}^4\text{He}(\alpha, p)$ results if one assumes that the lowest two states in ${}^7\text{Be}$ are mirror states of those in ${}^7\text{Li}$ and that the reaction mechanism is primarily compound-nuclear (see Sec. V). Since the incident channel ($\alpha + \alpha$) involves identical spinless particles, the compound-nucleus states in ${}^8\text{Be}$ must have even spin and parity. Then, since the final states in ${}^7\text{Be}$ and ${}^7\text{Li}$ have odd parity, the relative orbital angular momenta l in the $n + {}^7\text{Be}$ and $p + {}^7\text{Li}$ exit channels must be odd. The relative contribution from the various l -values in these channels of course depends on the structure of the ${}^8\text{Be}$, ${}^7\text{Be}$, and ${}^7\text{Li}$ states, but the likely shell-model configurations of these states as well as the large increase in the angular momentum barrier with l , suggests that the lowest allowed value, $l=1$, will be dominant. Then, since the assumption of charge symmetry requires the neutron and proton configurations of the ${}^8\text{Be}$ states to be identical, it follows that the total ${}^7\text{Be}$ production cross section is given by

$$\sigma_n = \sigma_{n_0} + \sigma_{n_1} = \frac{P_1^{n_0}}{P_1^{p_0}} \sigma_{p_0} + \frac{P_1^{n_1}}{P_1^{p_1}} \sigma_{p_1} \quad (3)$$

where σ_{n_0} and σ_{p_0} are the cross sections leading to the ground states of ${}^7\text{Be}$ and ${}^7\text{Li}$ respectively; and σ_{n_1} and σ_{p_1} , those leading to the first-excited states. The P_l are the penetrabilities in these various channels, defined by:²⁵

$$P_l = \frac{kR}{F_l^2 + G_l^2} \quad (4)$$

where k is the wave number; R , the channel radius; and F_l and G_l the Coulomb functions. The values of σ_n calculated using Eqs. (3) and (4) are shown in Fig. 8 for $E_\alpha \leq 43$ MeV, and qualitatively reproduce the magnitude

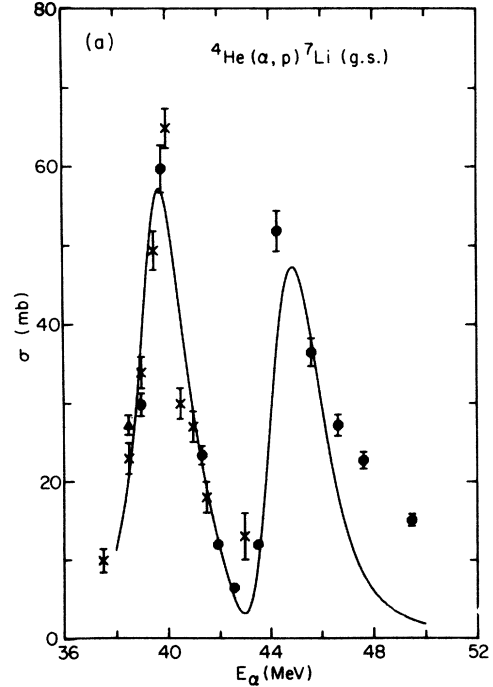


FIG. 5a. Comparison of the ${}^4\text{He}(\alpha, p){}^7\text{Li}(\text{g.s.})$ integral cross sections σ measured in the present study (circles) with those measured by Burcham *et al.*⁷ (triangles) and by Conzett *et al.*⁹ (crosses). The line represents the prediction for this cross section based on the ${}^8\text{Be}$ level parameters from the R-matrix fits of Kumar and Barker¹² to ${}^7\text{Li}(p, \alpha)$ cross sections.

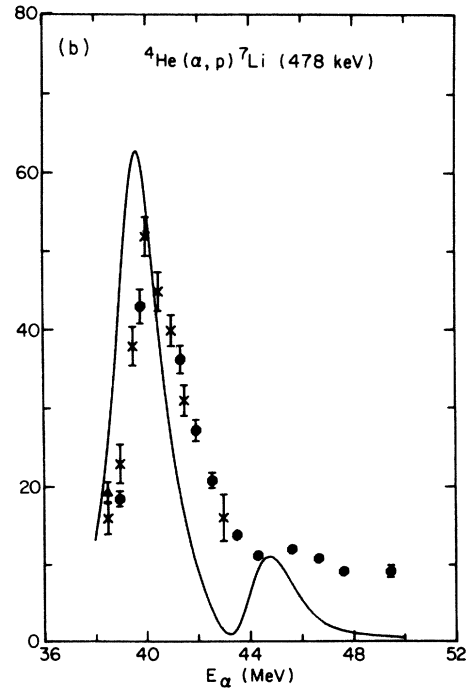


FIG. 5b. Comparison of measured and predicted integral cross sections for ${}^4\text{He}(\alpha, p)$ leading to the first excited state of ${}^7\text{Li}$. The symbols have the same meaning as in Fig. 5a.

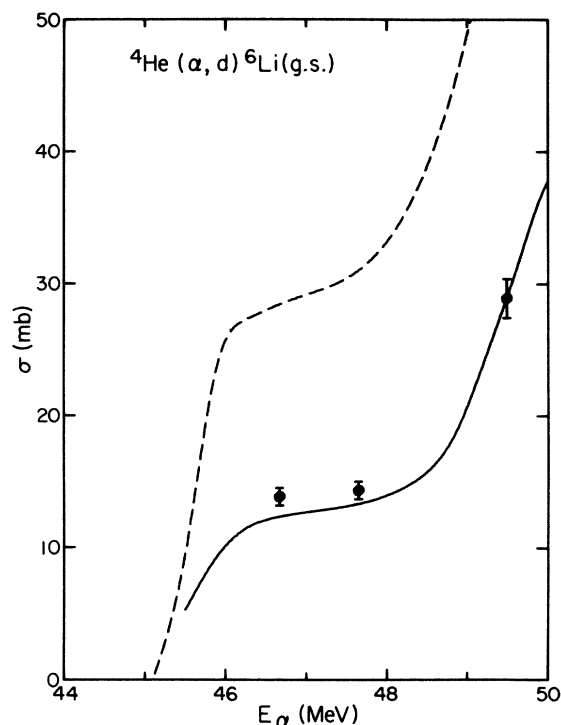


FIG. 6. Comparison of integral cross sections for the ${}^4\text{He}(\alpha, d){}^6\text{Li}(\text{g.s.})$ reaction leading to the ground state of ${}^6\text{Li}$ measured in the present study (circles) with detailed-balance predictions from the ${}^6\text{Li}(d, \alpha)$ cross section measurements of McClenahan and Segel²¹ (solid line) and those of Jeronimo *et al.*²² (dashed line).

and energy dependence of the ${}^4\text{He}(\alpha, n)$ data. The neutron cross sections are smaller than the proton cross sections in this energy region because $\ell=0$ is not allowed in the exit channels and the threshold energies for the neutron channels are significantly higher than those for the proton channels. Hence, near the neutron thresholds, the effects of the angular momentum dominate those of the Coulomb barrier and, since the channel energies are significantly smaller, the penetrabilities in the neutron channels are reduced. This point has apparently been overlooked in other work.⁸ The values of the penetrability determined from Eq. (4) are strongly dependent on the channel radius R ; however, as seen in Fig. 8, the ratios of the

TABLE II. $\alpha + \alpha \rightarrow n + {}^7\text{Be}$ Cross Sections.

E_α (MeV) (± 100 keV)	σ (mb)
39.43	26.3 ± 3.1
39.96	49.0 ± 4.7
41.67	40.3 ± 4.8
42.23	30.3 ± 3.0
43.00	22.6 ± 3.4
44.34	68.0 ± 6.2
44.52	72.9 ± 8.4
44.69	72.1 ± 6.3
47.36	35.1 ± 4.6

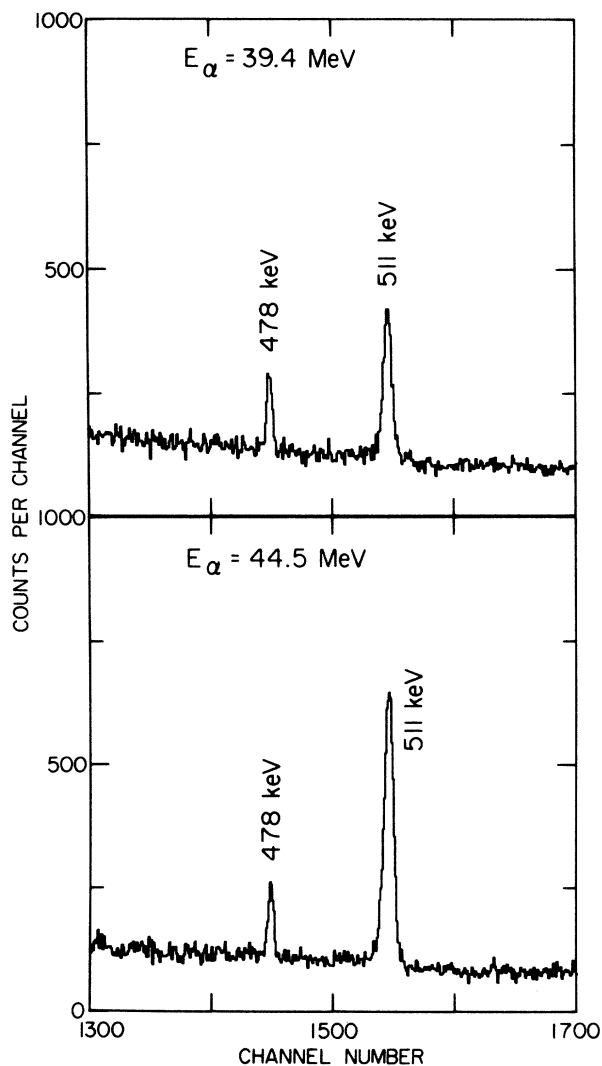


FIG. 7. γ -ray activity in the aluminum collecting foils 18 days and 16 days respectively after bombardment of the helium gas cell by 39.4 and 44.5 MeV α particles. The portions of the spectra are shown in the region of the 478 keV γ ray resulting from the ${}^7\text{Be}$ decay.

penetrabilities depend only weakly on R . It also should be pointed out that this model predicts a cross section at $E_\alpha=39$ MeV which is considerably larger than the upper limit of Walker, Link, and Smith,²⁴ suggesting that their measurement may be in error. For $E_\alpha > 43$ MeV, our measurements show that the ${}^7\text{Li}$ and ${}^7\text{Be}$ cross sections are essentially equal.

Finally, as has recently been suggested,⁸ these cross sections can be compared to the results of phase-shift analyses of $\alpha + \alpha$ elastic scattering, the elastic scattering phase-shifts allowing one to calculate the total reaction cross section. Below 39.6 MeV (the threshold for $\alpha + \alpha \rightarrow p + t + \alpha$), the only open reaction channels are the two lowest $p+{}^7\text{Li}$ and the two lowest $n+{}^7\text{Be}$ channels, precisely the channels for which we have measured the cross sections. Thus, up to $E_\alpha=39.6$ MeV the sum of our ${}^7\text{Li}$ and ${}^7\text{Be}$ production cross sections should be equal to the total reaction cross section for $\alpha + \alpha$, which can be compared directly with the phase-shift predictions. As

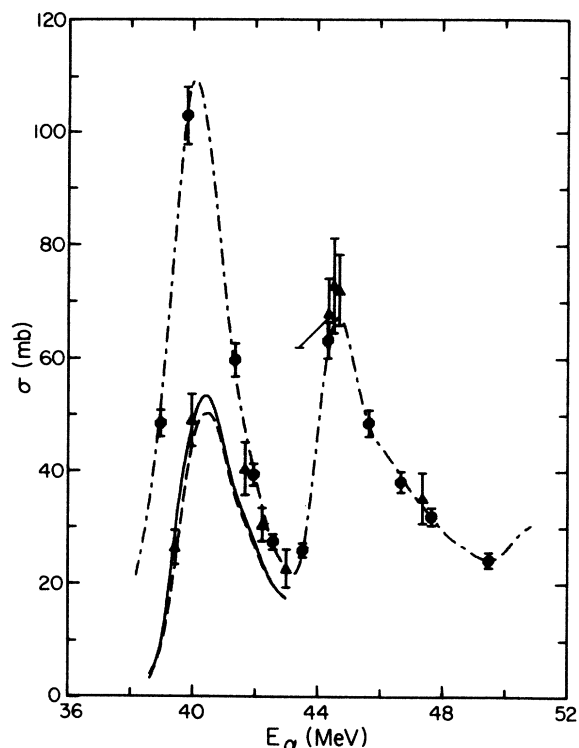


FIG. 8. Comparison between integral cross sections for ${}^7\text{Be}$ production (sum of ${}^4\text{He}(\alpha, n){}^7\text{Be}(\text{g.s.})$ and ${}^4\text{He}(\alpha, n){}^7\text{Be}(429 \text{ keV})$ cross sections) shown as triangles and those for ${}^7\text{Li}$ production (sum of ${}^4\text{He}(\alpha, p){}^7\text{Li}(\text{g.s.})$ and ${}^4\text{He}(\alpha, p){}^7\text{Li}(478 \text{ keV})$ cross sections) shown as circles. The solid line represents the prediction for the ${}^7\text{Be}$ production cross sections near threshold using Eq. (3) and a channel radius of 4.1 fm. The dashed line gives the prediction using a channel radius of 2.4 fm. (These predictions differ somewhat from those given in refs. 6 and 26 since in those references the difference between the ${}^7\text{Li}(\text{g.s.})$ and ${}^7\text{Li}(478 \text{ keV})$ thresholds were ignored). The dot-dashed line is to guide the eye through the ${}^7\text{Li}$ production cross section.

has been described elsewhere,^{2,6} the formula for the total reaction cross section σ_R when the identity of the α particles is properly accounted for is

$$\sigma_R = 2\pi\lambda^2 \sum_{\ell=0}^{\infty} (2\ell + 1) (1 - |e^{2i\delta_\ell}|^2),$$

even

where the δ_ℓ are the complex elastic-scattering phase shifts. As was shown in Ref. 26, our data agree reasonably well with phase-shift predictions up to the $\alpha + \alpha \rightarrow p + t + \alpha$ threshold energy, considering the uncertainties inherent in phase-shift analyses. Above this energy the phase-shift predictions exceed our summed cross sections, as is expected.

IV. THE ORIGIN OF ${}^7\text{Li}$ IN NATURE

A. Cosmic-ray spallation

The nuclei with $A < 12$ can be produced through spallation by high-energy ($> 1 \text{ MeV}$) particles if the environment

is sufficiently cool and low in density to prevent the products from being destroyed by further reactions. Reeves, Fowler, and Hoyle²⁷ suggested that such spallation reactions take place when cosmic rays permeating the galaxy strike particles in the interstellar medium and showed that this process could account for the observed abundances of ${}^6\text{Li}$ and the Be and B isotopes. However, the production of ${}^7\text{Li}$ seemed to be about an order of magnitude too low. This result was confirmed by the more complete calculations of Mitler⁴ and of Meneguzzi, Audouze, and Reeves.⁵

By far the most abundant nuclides in both cosmic rays and the interstellar medium are protons and alpha particles, with C, N, and O also present in significant numbers. Hence, the important reactions are $p+C, N, O$; $\alpha+C, N, O$; and $\alpha+\alpha$, with the $\alpha+\alpha$ reaction being especially important for the production of ${}^6\text{Li}$ and ${}^7\text{Li}$ because of the relatively high abundance of ${}^4\text{He}$. For a given nuclide i (such as ${}^7\text{Li}$) the number produced per unit time dn_i/dt is

$$\frac{dn_i}{dt} = \sum_{jk} n_k \int_{E_{jk}}^{\infty} \phi_j(E) \sigma_{jk}^i(E) dE,$$

where $\phi_j(E)$ is the flux per unit energy in the cosmic rays of nuclide j , $\sigma_{jk}^i(E)$ is the cross section for the production of i in the reaction $j+k$, n_k is the number of target nuclides k in the interstellar medium, and E_{jk} is the threshold energy for the reaction of $j+k$ leading to i . Integrating dn_i/dt over the age of the galaxy, one obtains the total production of the nuclide i .

In his calculations⁴ Mitler inferred the ${}^4\text{He}(\alpha, p)\text{Li}$ cross sections by means of the principle of detailed balance from ${}^7\text{Li}(p, \alpha)$ measurements (using those of Mani *et al.*¹⁵ at low energies), assumed that the ${}^4\text{He}(\alpha, n){}^7\text{Be}$ cross sections were equal to the ${}^4\text{He}(\alpha, p)\text{Li}$ cross sections, and ignored the production of ${}^7\text{Be}$ and ${}^7\text{Li}$ in their first excited states. With these assumptions Mitler calculated that 58% of the ${}^7\text{Li}$ production arises from the $\alpha+\alpha$ reaction alone. We have repeated this calculation using the same abundances and cosmic-ray spectral shape as Mitler but with the cross sections determined from the present measurements and those of King *et al.*⁶ up to 140 MeV. These cross sections are consistent with an exponential dependence for $E_\alpha > 70 \text{ MeV}$ and thus we have assumed an exponential extrapolation beyond 140 MeV. (Assuming a constant cross section beyond 200 MeV changes the results of the calculations by only a few per cent.) Using Mitler's value for the fraction of ${}^7\text{Li}$ ions surviving while stopping in the interstellar medium, we find that the ${}^7\text{Li}$ production from the $\alpha+\alpha$ reaction is reduced to 52% of that Mitler obtained and that the total ${}^7\text{Li}$ production is lowered by 27%.

Assuming a cosmic-ray flux constant in time and estimating the loss of the products through further reactions and escape from the galaxy, Mitler calculated abundances for ${}^6\text{Li}$, ${}^9\text{Be}$, ${}^{10}\text{B}$, and ${}^{11}\text{B}$ which were within a factor of 2 of the observed abundances. Including effects of a cosmic-ray flux which decreases over the galactic lifetime and of the destruction of Li, Be, and B through astration, Mitler found ${}^6\text{Li}$, ${}^9\text{Be}$, ${}^{10}\text{B}$, and ${}^{11}\text{B}$ abundances even closer to those observed. In both cases, however, the calculated ${}^7\text{Li}/\text{H}$ abundance ratio was almost an order of magnitude smaller than the observed value²⁸ (based on meteorite observations) of 1.4×10^{-9} . Using our new measurements of the $\alpha+\alpha$ cross sections increases the magnitude of this discrepancy.

The calculations of Meneguzzi, Audouze, and Reeves⁵ involve a more self-consistent approach to the problem. Beginning with a model for the source cosmic-ray flux, they calculated both the change in the cosmic-ray flux as well as the interstellar medium from interactions as the

cosmic rays propagate through the galaxy. The resulting cosmic-ray spectrum below 100 MeV/nucleon is in disagreement with and much smaller than Mitler's assumption. Hence, in this model the low energy region contributes much less to the total ${}^7\text{Li}$ production and thus the use of the present cross sections and those of Ref. 6 would have less effect on the ${}^7\text{Li}$ production rate in the $\alpha+\alpha$ reaction. Unfortunately, modulation effects of the solar wind greatly complicate terrestrial observations of the galactic cosmic-ray spectrum in this energy region so that it is difficult to determine which of the two assumptions is correct.^{4,5} Although the model of Meneguzzi, Audouze, and Reeves differs in many details from that of Mitler, they also found good agreement with observations for the ${}^6\text{Li}$, ${}^9\text{Be}$, ${}^{10}\text{B}$, and ${}^{11}\text{B}$ abundances, and again the ${}^7\text{Li}$ abundance was about an order of magnitude too small (${}^7\text{Li}/\text{H}=1.2\times 10^{-9}$).

Another way to consider the ${}^7\text{Li}$ problem is to determine the ${}^7\text{Li}/{}^6\text{Li}$ abundance ratio. ${}^6\text{Li}$ production is also considerably influenced by the $\alpha+\alpha$ reaction. However, the present measurements for ${}^4\text{He}(\alpha, d){}^6\text{Li}$ are in reasonable agreement with those used in Refs. 5 and 6. Although no data are available for the three-body channels leading to ${}^6\text{Li}$, it seems probable that the actual ${}^6\text{Li}$ production cross sections are similar to those assumed in the calculations. Using these cross sections, Meneguzzi *et al.* calculated a ${}^7\text{Li}/{}^6\text{Li}$ abundance ratio of 1.5; and Mitler, a ratio of 2.0. (Our modification of Mitler's ${}^7\text{Li}$ calculation yields a ratio of 1.4.) Very few extraterrestrial observations of this ratio have been made; however, the galactic ${}^7\text{Li}/{}^6\text{Li}$ abundance ratio is not believed^{28,29} to differ significantly from the terrestrial value of 12.5.

Thus, both the ${}^7\text{Li}$ abundance alone and also the ${}^7\text{Li}/{}^6\text{Li}$ abundance ratio imply that production of ${}^7\text{Li}$ by standard models of spallation by galactic cosmic rays is deficient by about an order of magnitude. This strongly suggests^{29,30} the need to consider other ways to produce ${}^7\text{Li}$.

B. Alternative ${}^7\text{Li}$ production mechanisms

Because of the low thresholds of the $p+{}^{14}\text{N}$ reactions and the large cross sections for the $\alpha+\alpha$ reactions near their thresholds, a process which yields large fluxes of particles in the neighborhood of a few tens of MeV/nucleon or less would substantially affect the production of Li, Be, and B. Recently Bodansky, Jacobs, and Oberg³¹ concluded that a suitably chosen flux of particles with energies less than 25 MeV/nucleon can reproduce not only the observed ratio of the Li abundance to that of B and Be, but also the observed ${}^7\text{Li}/{}^6\text{Li}$ ratio as well. (It should be noted that although Bodansky *et al.* assumed cross sections for the ${}^7\text{Li}$ production in the $\alpha+\alpha$ reaction which are too large, their general conclusion is not altered by the use of the cross sections determined in this work and those at higher energies from Ref. 6.)

It has been suggested³² that the shock waves accompanying a supernova explosion could produce protons, helium, and C, N, and O nuclei with approximately 10 MeV/nucleon and thus could produce^{29,32} Li, Be, and B. However, whether such high-energy particles actually do occur in significant quantities is still in doubt.^{29,33} Because of the lack of direct observational data on galactic cosmic rays below 100 MeV/nucleon, it has also been suggested that an intense low-energy component may be present in the cosmic rays which could alter the relative production of the Li, Be, and B isotopes.^{5,34,35} Again, however, no specific model yielding the required flux of low-energy cosmic rays has yet been devised.

In addition to these low-energy spallation mechanisms, it has been suggested³⁶ that the ${}^3\text{He}(\alpha, \gamma){}^7\text{Be}$ reaction may

proceed rapidly enough in red giant stars so that significant amounts of ${}^7\text{Be}$ might be transported to cooler regions of the star. Then the ${}^7\text{Li}$ resulting from the ${}^7\text{Be}$ decay would be less likely to be destroyed. This model could account for large Li/H ratios observed³⁷ in some red giants, but it is uncertain^{29,30,38} whether such a process could explain the cosmic abundance of ${}^7\text{Li}$.

It was demonstrated by Wagoner, Fowler, and Hoyle³ that ${}^3\text{He}(\alpha, \gamma){}^7\text{Be}$ and ${}^3\text{H}(\alpha, \gamma){}^7\text{Li}$ form an important part of the nuclear reaction network during the big bang. This causes significant amounts of ${}^7\text{Li}$ to be produced together with ${}^2\text{H}$, ${}^3\text{He}$, and ${}^4\text{He}$. It is widely believed that nucleosynthesis during the big bang accounts for the observed abundance of ${}^4\text{He}$, and recently it has been suggested that most of the observed ${}^2\text{H}$ originated in this process as well. The amount of ${}^2\text{H}$ produced in a big bang is a very sensitive function of the average baryon density of the universe ρ_b , with production increasing as the density is decreased. Hence, if it is assumed that all the deuterium is made in the big bang, one can set an upper limit on ρ_b . This limit implies an open universe.^{23,39}

The amount of ${}^7\text{Li}$ produced in the big bang is also relatively sensitive to ρ_b .^{3,39} As is discussed elsewhere,⁴⁰ the assumption that all ${}^7\text{Li}$ has been produced in the big bang and the neglect of astration also leads to a limit on ρ_b which implies an open universe and, considering the uncertainties in the observed abundances, is reasonably consistent with the limit set by the deuterium abundance. Moreover, since the production of ${}^7\text{Li}$ tends to increase as the ρ_b is increased,^{3,39} this limit would be lowered if alternative production mechanisms for ${}^7\text{Li}$ should become established, thus improving the agreement with the deuterium limit.

V. THE STRUCTURE OF ${}^8\text{Be}$ BETWEEN 19 AND 25 MeV

A number of known ${}^8\text{Be}$ states lie within the excitation energy region (19-25 MeV) covered in the present experiments. The ${}^4\text{He}(\alpha, p)$ and ${}^4\text{He}(\alpha, n)$ excitation functions have considerable structure and it is reasonable to interpret these in terms of compound nucleus states in ${}^8\text{Be}$. Since $\alpha+\alpha$ is the entrance channel for the reactions of concern here, the ${}^8\text{Be}$ states involved must have even spin and parity. Ajzenberg-Selove and Lauritsen¹⁰ cite six such states in this excitation energy region: a $J^\pi, T=4^+, 0$ state at 19.9 MeV; a $2^+, 0$ state at 20.1 MeV; a $0^+, 0$ state at 20.2 MeV; a $2^+, 0$ state at 22.2 MeV; a $2^+, 0$ state at 25.2 MeV; and a $4^+, 0$ state at 25.5 MeV.

The $\alpha+\alpha+p+{}^7\text{Li}(\text{g.s.})$ excitation function (Figs. 3 and 5(a)) has two large peaks, one near $E_\alpha=40$ MeV and another near $E_\alpha=44.5$ MeV. It is natural to interpret the first of these peaks as resulting from the cluster of ${}^8\text{Be}$ states near 20 MeV excitation energy (in fact, analysis of the angular distribution coefficients shows^{10,12} that the 2^+ state at 20.1 MeV dominates) and the second peak as resulting from the 2^+ state at 22.2 MeV. On the other hand, the $\alpha+\alpha+p+{}^7\text{Li}(478\text{ keV})$ excitation function (Figs. 3 and 5(b)) has only one large peak which occurs slightly above the first resonance in the $\alpha+\alpha+p+{}^7\text{Li}(\text{g.s.})$ excitation function. The cross section also falls much more slowly on the high energy side of the peak than is the case for the $\alpha+\alpha+p+{}^7\text{Li}(\text{g.s.})$ reaction.

Kumar and Barker¹² have analyzed the ${}^7\text{Li}(p, \alpha)$ data from studies involving both unpolarized and polarized protons up to $E_p=7$ MeV using an R-matrix approach. (It should be noted that Kumar and Barker divided the cross sections of Ref. 15 by 2 and thus are in accord with our ground-state cross sections.) Kumar and Barker were able to fit these data reasonably well by including six $T=0$ states in ${}^8\text{Be}$: two $J^\pi=0^+$ states at 19.7 and 21.8 MeV and

four $J^\pi=2^+$ states at 15.9, 20.1, 22.2, and 25.0 MeV. In addition to the $\alpha + \alpha$ and $p + {}^7\text{Li}(\text{g.s.})$ channels, the $p + {}^7\text{Li}(478 \text{ keV})$, $n + {}^7\text{Be}(\text{g.s.})$, and $n + {}^7\text{Be}(429 \text{ keV})$ channels were included in the calculation. Isospin was assumed to be a good quantum number so that the reduced widths in the neutron channels were equal to those in the analogous proton channels. Good fits to the cross sections and $L=2$ angular-distribution and analyzing-power coefficients were obtained by restricting the orbital angular momentum in the proton channels to $\ell=1$. (This corresponds to restricting the odd parity orbitals of the ${}^8\text{Be}$ shell model configurations to be p orbitals.) In order to fit the $L=4$ and $L=6$ coefficients, however, $\ell=3$ was required in the $p+{}^7\text{Li}(\text{g.s.})$ and the analogous $n+{}^7\text{Be}(\text{g.s.})$ channels (corresponding to the addition of f-orbital admixtures in the shell model configurations).

Since only data for the ${}^7\text{Li}(p,\alpha)$ reaction were included, the fit of Kumar and Barker was not particularly sensitive to the reduced widths for the $p+{}^7\text{Li}(478 \text{ keV})$ channel. However, it is of interest to see how well these parameters fit the $\alpha + \alpha + p+{}^7\text{Li}(478 \text{ keV})$ data. Using the Kumar and Barker formalism and the level parameters obtained in their fit to the ${}^7\text{Li}(p,\alpha)$ data, we have calculated the cross sections for the $\alpha + \alpha + p+{}^7\text{Li}(\text{g.s.})$ and $\alpha + \alpha + p+{}^7\text{Li}(478 \text{ keV})$ reactions. The results are shown in Figs. 4 and 5. The fits to the ground state data are good up to about 46 MeV (corresponding to the limit of the ${}^7\text{Li}(p,\alpha)$ data included in the Kumar-Barker fit). Some adjustments in the parameters, however, are clearly required in order to fit the data for the 478 keV state. In particular, the predicted strength of the 40 MeV resonance is too large and the cross section is predicted to fall much too sharply beyond this resonance. This feature may be due to interference between the 2^+ levels at 20.1 and 22.2 MeV and adjustment of the magnitudes and signs of the reduced widths of these levels might improve the fit to the data; however, an additional ${}^8\text{Be}$ level near 21 MeV might also be required. The B_2 coefficient is also poorly reproduced at all energies.

Because the orbital angular momentum of the $p+{}^7\text{Li}(478 \text{ keV})$ channel was restricted to $\ell=1$, the B_4 coefficient is predicted to be zero (Fig. 4(b)). This assumption is not in significant disagreement with the data below 44 MeV; however, above this energy, B_4 becomes quite large, indicating a contribution from $\ell=3$ reduced widths, or equivalently f-orbital admixtures in the shell model wavefunctions. More thorough calculations are required before any firm conclusions concerning the structure of ${}^8\text{Be}$ can be drawn from our data, but the Kumar-Barker parameters are clearly inadequate.

VI. SUMMARY

We have measured differential cross sections for ${}^4\text{He}(\alpha, p){}^7\text{Li}(\text{g.s.})$ and ${}^4\text{He}(\alpha, p){}^7\text{Li}(478 \text{ keV})$ and the integral cross sections for ${}^4\text{He}(\alpha, n){}^7\text{Be}(\text{g.s.}+429 \text{ keV})$ between 39 and 50 MeV. The absolute cross sections for ${}^4\text{He}(\alpha, p){}^7\text{Li}(\text{g.s.})$ were found to be consistent using the principle of detailed balance with the most recent determinations^{14,13} of the ${}^7\text{Li}(p,\alpha)$ cross sections. The ${}^4\text{He}(\alpha, p){}^7\text{Li}(\text{g.s.}+478 \text{ keV})$ and ${}^4\text{He}(\alpha, n){}^7\text{Be}(\text{g.s.}+429 \text{ keV})$ integral cross sections were found to be essentially identical above 43 MeV. Below this energy the ${}^7\text{Be}$ cross sections are lower because of the higher threshold for ${}^7\text{Be}$ reactions. In addition, below the first three-body threshold, the sum of the ${}^7\text{Be}$ and ${}^7\text{Li}$ reactions is consistent with the total reaction cross sections implied by $\alpha + \alpha$ phase shifts.

The ${}^4\text{He}(\alpha, p)$ and ${}^4\text{He}(\alpha, n)$ reactions contribute to the production of ${}^7\text{Li}$ in the galaxy through spallation of the interstellar medium by cosmic rays, and our measurements indicate that the cross sections which have been assumed for these reactions in calculations^{4,5} of the spallation process are too large. This confirms earlier conclusions^{4,5,29,30} that spallation by galactic cosmic rays alone cannot account for the observed abundance of ${}^7\text{Li}$. Other ${}^7\text{Li}$ production mechanisms have been proposed which utilize the ${}^4\text{He}(\alpha, p)$ and ${}^4\text{He}(\alpha, n)$ reactions in the energy range of our measurements, such as supernova shock waves and low-energy cosmic rays. Although our cross section measurements should have a significant effect on calculations of ${}^7\text{Li}$ production from such processes, it is still too early to judge whether these processes could possibly account for the universal ${}^7\text{Li}$ abundance. A possible simple alternative is to assume that most of the ${}^7\text{Li}$ in the universe was created in the big bang, as seems likely² for ${}^4\text{He}$ and ${}^2\text{H}$. This assumption requires a universal baryon density which is reasonably consistent with conclusions based on requirements of ${}^2\text{H}$ production² and implies that the universe is open.

Finally, we have used the parameters from R-matrix fits of Kumar and Barker¹² to ${}^7\text{Li}(p,\alpha)$ data to predict the cross sections for ${}^4\text{He}(\alpha, p){}^7\text{Li}(478 \text{ keV})$. These calculations do not fit the data, indicating that some adjustments of the level parameters are required.

The authors would like to thank Prof. V.E. Viola, Jr. and Dr. G.J. Mathews for useful discussions regarding this work and Prof. F.C. Barker for providing helpful information concerning his R-matrix calculations.

*Research supported by the National Science Foundation.

†Present address: Hahn-Meitner-Institut für Kernforschung, Berlin GmbH, 1 Berlin-West 39, Germany.

¹E.M. Burbidge, G.R. Burbidge, W.A. Fowler, and F. Hoyle, *Rev. Mod. Phys.* **29**, 547 (1957). Some more recent references are given in V. Trimble, *Rev. Mod. Phys.* **47**, 877 (1975).

²J.R. Gott, J.E. Gunn, D.N. Schramm, and B.M. Tinsley, *Astrophys. J.* **194**, 543 (1974); R.I. Epstein, J.M. Lattimer, and D.N. Schramm, *Nature* **263**, 198 (1976); D.N. Schramm and R.V. Wagoner, *Ann. Rev. Nucl. Sci.*, to be published.

³R.V. Wagoner, W.A. Fowler, and F. Hoyle, *Astrophys. J.* **148**, 3 (1967).

⁴H.E. Mitler, *Astrophys. Space Sci.* **17**, 186 (1972) and Smithsonian Astrophysical Observatory Special report No. 330 (1970).

⁵M. Meneguzzi, J. Audouze, and H. Reeves, *Astron. and Astrophys.* **15**, 337 (1971).

⁶C.H. King, H.H. Rossner, S.M. Austin, W.S. Chien, G.J. Mathews, V.E. Viola, Jr., and R.G. Clark, *Phys. Rev. Lett.* **35**, 988 (1975).

⁷W.E. Burcham, G.P. McCauley, D. Bredin, W.M. Gibson, D.J. Prowse, and J. Rotblat, *Nucl. Phys.* **5**, 141 (1958).

⁸R.J. Slobodrian, *Phys. Lett.* **63B**, 5 (1976).

⁹H.E. Conzett, R.J. Slobodrian, S. Yamabe, and E. Shield, *Compte Rendu du Congrès International de Physique Nucléaire, Paris (1964)*, P. Gugenberger, ed. (Centre National de la Recherche Scientifique, Paris, 1964), p. 228.

¹⁰F. Ajzenberg-Selove and T. Lauritsen, *Nucl. Phys.* **A227**, 1 (1974).

¹¹G.M. Lerner and J.B. Marion, *Nucl. Inst. Meth.* **69**, 115 (1969).

- ¹²N. Kumar and F.C. Barker, Nucl. Phys. A167, 434(1971).
- ¹³F.C. Barker, Astrophys. J. 173, 477(1972).
- ¹⁴Y. Cassagnou, J.M.F. Jeronimo, G.S. Mani, A. Sadeghi, and P.D. Forsyth, Nucl. Phys. 33, 449(1962).
- ¹⁵G.S. Mani, R. Freeman, F. Picard, A. Sadeghi, and D. Redon, Nucl. Phys. 60, 588(1964).
- ¹⁶J.M. Freeman, R.C. Hanna, and J.H. Montague, Nucl. Phys. 5, 148(1958).
- ¹⁷K. Kilian, G. Clausnitzer, W. Dürr, D. Fick, R. Fleischmann, and H.M. Hofmann, Nucl. Phys. A126, 529(1969).
- ¹⁸M.S. Goldberger and K.M. Watson, Collision Theory (Wiley, New York, 1964) p. 169.
- ¹⁹S. de Benedetti, Nuclear Interactions (Wiley, New York, 1964) p. 329.
- ²⁰W.A. Fowler, G.R. Caughlin, and B.A. Zimmerman, Ann. Rev. Astron. Ap. 5, 525(1967).
- ²¹C.R. McClenahan and R.E. Segel, Phys. Rev. C 11, 370(1975).
- ²²J.M.F. Jeronimo, G.S. Mani, F. Picard, and A. Sadeghi, Nucl. Phys. 38, 11(1962).
- ²³Standard reference material 4215, National Bureau of Standards, U.S. Department of Commerce.
- ²⁴D. Walker, W.T. Link, and W.I.B. Smith, Proc. Phys. Soc. A65, 861(1952).
- ²⁵A.M. Lane and R.G. Thomas, Rev. Mod. Phys. 30, 257(1958).
- ²⁶C.H. King, Sam M. Austin, W.S. Chien, and H.H. Rossner, Phys. Lett. 67B, 389(1977).
- ²⁷H. Reeves, W.A. Fowler, and F. Hoyle, Nature 226, 727(1970).
- ²⁸A.G.W. Cameron, Space Sci. Rev. 15, 121(1973).
- ²⁹H. Reeves, Ann. Rev. Astron. Astrophys. 12, 437(1974).
- ³⁰H. Reeves, J. Audouze, W.A. Fowler, and D.N. Schramm, Astrophys. J. 179, 909(1973).
- ³¹D. Bodansky, W.W. Jacobs, and D.L. Oberg, Astrophys. J. 202, 222(1975).
- ³²S.A. Colgate, Astrophys. J. 187, 321(1974) and 195, 493(1975); J. Audouze and J.W. Truran, Astrophys. J. 182, 839(1973); R.I. Epstein, W.D. Arnett, and D.N. Schramm, Astrophys. J. 190, L13 (1974) and Astrophys. J. (Suppl.) 31, 111(1976).
- ³³T.A. Weaver and G.F. Chapline, Astrophys. J. 192, L57(1974); T.A. Weaver, Astrophys. J. (Suppl.) 32, 233(1976).
- ³⁴R. Canal, J. Isern, and B. Sanahuja, Astrophys. J. 200, 646(1975).
- ³⁵C.T. Roche, R.G. Clark, G.J. Mathews, and V.E. Viola, Jr., Phys. Rev. C 14, 410(1976).
- ³⁶A.G.W. Cameron and W.A. Fowler, Astrophys. J. 167, 111(1971); J.M. Scalo and R.K. Ulrich, Astrophys. J. 183, 151(1973); I.-J. Sackmann, R.L. Smith, and K.H. Despain, Astrophys. J. 187, 555(1974).
- ³⁷G. Wallerstein and P.S. Conti, Ann. Rev. Astron. Astrophys. 7, 99(1969); A.M. Boesgaard, Astrophys. J. 161, 1003(1970).
- ³⁸J. Audouze and B.M. Tinsley, Astrophys. J. 192, 487(1974).
- ³⁹R.V. Wagoner, Astrophys. J. 179, 343(1973).
- ⁴⁰Sam M. Austin and C.H. King, Nature, to be published.